Chalcogenide Letters Vol. 8, No. 8, August 2011, p. 453-467

KINETICS OF NON-ISOTHERMAL CRYSTALLIZATION OF TERNARY $Se_{85}Te_{15-x}Sb_x$ GLASSY ALLOYS

I.S. YAHIA[a*], A.M. SHAKRA [a], M. FADEL [a], N.A. HEGAB [a], A.M. SALEM [b], A.S. FARID [a]

[a]*Physics Department, Faculty of Education, Ain Shams University, Cairo, Egypt*

[b]*Physics Division, Electron Microscopy and Thin Film Laboratory, National Research Center, Dokki, Cairo, Egypt.*

Bulk glasses of $Se_{85}Te_{15-x}Sb_x$ (x=0,2,4&6at.wt%) are prepared by melt quenching technique. The amorphous nature of bu`lk samples was detected by X-ray diffraction analysis. This paper presents the results of kinetics studies of glass transition and crystallization kinetics of phase transformation by non-isothermal method using differential scanning calorimetry (DSC) technique for the investigated compositions .DSC is performed at different heating rates. The values of glass transition and crystallization temperatures are found to be composition and heating-rate dependent. The obtained results have been analyzed in terms of the activation energy of the glass transition E_g using Kissinger's and Mahadevan et al relations. Values of E_g obtained by the two relations are agreement with each other. The growth kinetics and its dimensionality have been investigated using three different models viz. Kissinger, Augis et al and Mahadevan equations. It is found that the activation energy for crystallization E_c increases with Sb content which indicated that the speed of crystallization rate is faster with increasing Sb content. The results indicate that the crystallization process is two-dimensional growth.

(Received June 14, 2011; Accepted August 01, 2011)

Keywords: Chalcogenide glasses, Crystallization kinetics of Se-Te-Sb.

1. Introduction

Impressive progress has been made over the last two decades in our understanding of the structure of semiconducting chalcogenide glasses from the theoretical, as well as experimental point of view [1]. Chalcogenide glasses are well-known and promising materials for a variety of photonic applications such as ultra fast optical switches, frequency converters, optical amplifiers, infrared lasers, and infrared transmitting optical fibers. The interest in these materials stems principally from their low phonon energy, extended infrared transparency, high refractive index, high photosensitivity, ease of fabrication and processing, good chemical durability, and special second/third order optical non-linearity [2]. Two different approaches have been adapted to investigate these materials: The first is the analysis of their structure and physical properties, while the second is connected with their stability, i.e. the study of glass transformation and crystallization process. Since the amorphous state is essentially a metastable one, it possesses the possibility of transformation into a more stable crystalline state. The most promising properties of chalcogenide glasses have been found to deteriorate drastically during crystallization. Understanding the mechanisms of crystallization to impede or control crystallization is therefore a prerequisite for most applications, as stability against crystallization determines their effective working limits [3-7].

* Corresponding author: abir_net_2005@hotmail.com

Two popular techniques have been widely employed for the study of the crystallization behavior of glasses upon heating, isothermal and non-isothermal crystallization analysis [8-12]. In the isothermal method the sample is brought quickly to a temperature above the glass transition T_g, and the heat evolving during the crystallization process at a constant temperature is recorded as a function of time. In the non-isothermal method, the sample is heated at a fixed rate β (^oC/min), and the heat evolving is recorded as a function of temperature or time [4,13,14]. Non-isothermal analysis of the crystallization kinetics, of metallic glasses and glass forming liquid, has become increasingly attractive. Compared with isothermal techniques, non-isothermal experiments can be performed over a shorter time period and over a wider temperature range.

Thermal analysis methods including differential thermal analysis (DTA) and differential scanning calorimetry (DSC) are particularly important as they: (i) are easy to carry out, (ii) require little sample preparation, (iii) are quite sensitive and (iv) are relatively independent of the sample geometry. DSC is the more sensitive of the two calorimetric techniques and measures the volume fraction transferred as a function of time and temperature by measuring the heat liberated or absorbed during the phase change [15,16].

Chalcogenide glasses containing Se-Te belonging to VIB group elements are efficient materials for thin film circuits, fabrication of semiconductor glasses, transistors, detectors and other practical applications. From a technological point of view, these glasses should be thermally stable with time and temperature during use. However, thermal instability leading to crystallization is found to be one of the drawbacks of these glasses. Thus several attempts[17] have been already been made to improve the stability of Se-Te by the addition of third element such as Bi, Sb, Ge, In, Ag and others[18].Such addition to Se-Te glass converts it into an interesting material and new promising properties of the material are expected[19]. It is found that the addition of Sb to Se-Te is expected to create the compositional and configurationally disorder as compared to binary alloy.

The aim of work is to study the crystallization kinetics of amorphous $Se_{85}Te_{15-x}Sb_x$ (x=0, 2,4,&6at.wt%)glassy system using the DSC technique under non-isothermal conditions with the sample heated at several uniform heating rates. The study of kinetics is always connected with the concept of activation energies. Values of the activation energies of crystallization are determined for the study compositions. The glass transition temperature, crystallization temperature at different heating rates and structural change during glass transition have been determined. The glass transition temperature (T_g), peak crystallization temperature T_p, the activation for glass transition E_g and the activation energy of crystallization E_c and the dimensionality parameter n(Avrami exponent) are calculated at different heating rates by using different kinetics models to investigate the growth process in the transformation .The heating rate dependence and composition dependence of the activation energies of glass transition and crystallization are discussed.

2. Experimental details

Se_{85} Te_{15-x} Sb_x compositions glassy (x=0,2,4&6at.wt%) are prepared by melt quenching technique. The elementary constituents of each composition of purity 99.999 % were weighted in accordance with their atomic percentage and loaded in a pre cleaned silica tubes. The tubes with their constituent elements (5 gm total in weight) were sealed in a vacuum of 10^{-5} Torr. The tube was placed in an oscillatory furnace where the temperature was increased at the rate of 2-3^{0}C/min and heated regularly to 850^{0}c to allow Se, Te and Sb to react completely. The ampoule was frequently rocked for 12h at the maximum temperature to make the melt homogenous then quenched in ice water very rapidly. Quenched samples were removed from the tubes by breaking the silica tubes. The initial vitreous alloys were powdered and separated according to the size. The chemical composition of the investigated samples was checked by energy dispersive X-ray analysis (EDX) using JOEL 5400 scanning electron microscope. The structural identification of the investigated glassy compositions was confirmed by both X-ray diffraction XRD using Philips X-ray unit (PW3710) with generator (PW 1830) supplied with a copper target with Ni filter. The X-ray tube was operated at 40 kV and 30 mA.

The thermal behavior was investigated using differential scanning caliometry DSC (Shimadzu DSC-50). Typically, 20 mg of sample in powder form was sealed in standard aluminum pans and heated at different rates ranging from 2.5 to 40 ^{o}C/min. The accuracy of the heat flow is ± 0.01 mW/cm and the temperature precision as determined by the microprocessor of the thermal analyzer is ± 0.1 ^{0}C, with an average standard error of about± 1^{0}C.

3. Results and Discussions

3.1. Structure identification

3.1.1 X-ray diffraction patterns XRD

X-ray diffraction pattern was carried out for Se_{85} Te_{15-x} Sb_x (x=0,2,4&6at.wt%) system in powder form and shown in Fig. (1). The results indicate that the prepared samples are of amorphous nature due to the absence of sharp peaks and the presence of only broad humps.

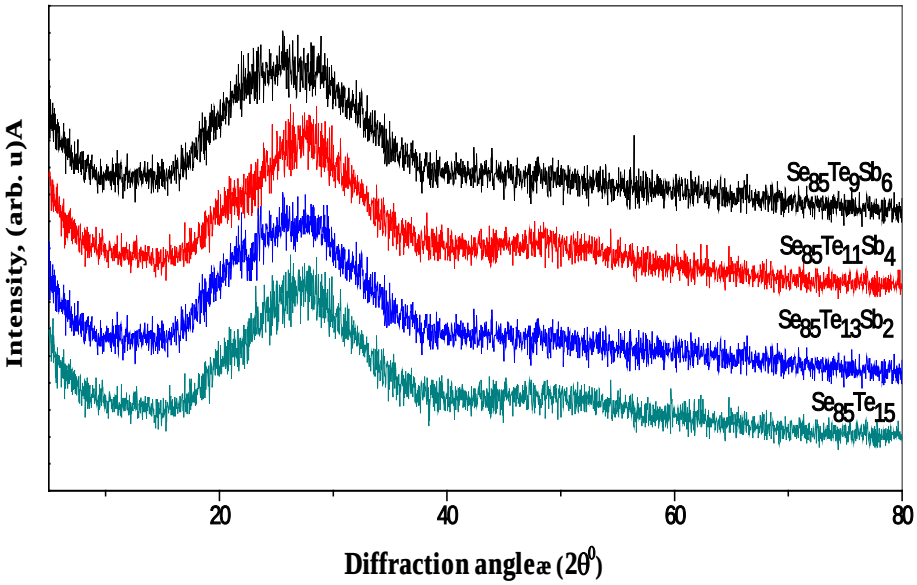

Fig. (1) X-ray diffraction patterns for $Se_{85}Te_{15-x}Sb_x$ (x = 0,2,4&6 at.wt%) in powder form.

3.1.2. Electron Dispersive X-ray Spectrum analysis (EDX)

Composition of the investigated samples was checked by energy dispersive X-ray spectrum analysis using a scanning electron microscope. The obtained data showed that the percentage of the constituent elements of the studied compositions are approximately the same as tabulated in Table1.

Table 1. Eneregy dispersive X-ray analysis (EDX) for $Se_{85}Te_{15-x}Sb_x$ films.

Calculated composition	At % (Experimental)			Nominal compositions
	Se	Te	Sb	
$\mathbf{Se_{85}Te_{15}}$	82.46	17.54	-	$Se_{82.46}Te_{17.54}$
$\mathbf{Se_{85}Te_{13}Sb_2}$	83.73	14.40	1.87	$Se_{83.73}Te_{14.4}Sb_{1.87}$
$\mathbf{Se_{85}Te_{11}Sb_4}$	83.79	10.85	5.36	$Se_{83.79}Te_{10.85}Sb_{5.36}$
$\mathbf{Se_{85}Te_9Sb_6}$	84.41	8.12	7.47	$Se_{84.41}Te_{8.12}Sb_{7.47}$

3.2. Thermal analysis

The crystallization studies have been made under non-isothermal conditions with the sample heated at several uniform rates.

A typical DSC trace of $Se_{85}Te_{15}$ obtained at a heating rate β of 10 ^{o}C/min, is given in Fig. (2), as a representative example. This figure shows three characteristic phenomena (endothermic and exothermic peak), which are resolved in the temperature region studied. The first one is the endothermic peak, at the glass transition temperature (T_g) ,which arise due to an abrupt increase in the specific heat of the sample. The second is exothermic peak associated with maximum crystallization rate at temperature (T_p), while the third transition is an endothermic peak due to melting (T_m).

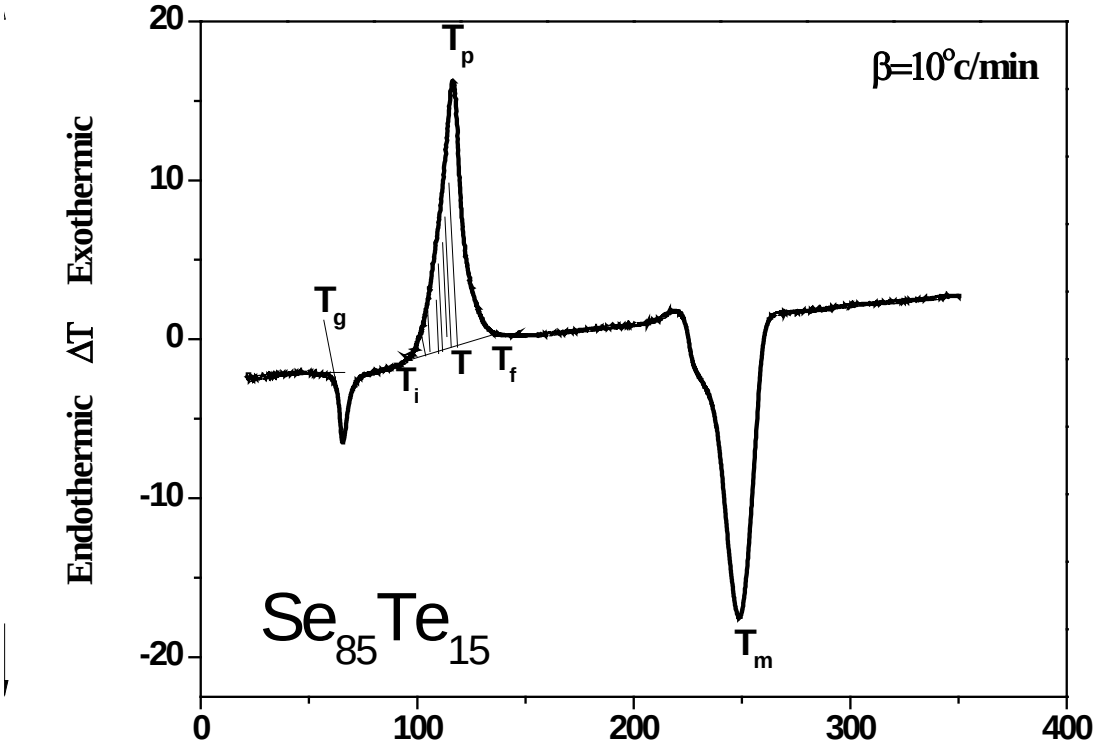

Fig.(2) Typical DSC trace of $Se_{85}Te_{15}$ at a heating

A complete set of DSC thermograms, measured at different heating rates for $Se_{85}Te_{13}$ Sb_2, $Se_{85}Te_{11}$ Sb_4 glasses as examples at different heating rates (β =2.5,5,10,20 and 40 ^{o}C/min) are shown in Figs.3 (a,b).It is observed that both T_g and T_p shift towards higher temperature as heating rate is increased. The values of T_g and T_p for the compositions under investigation are listed in Table 2**.**

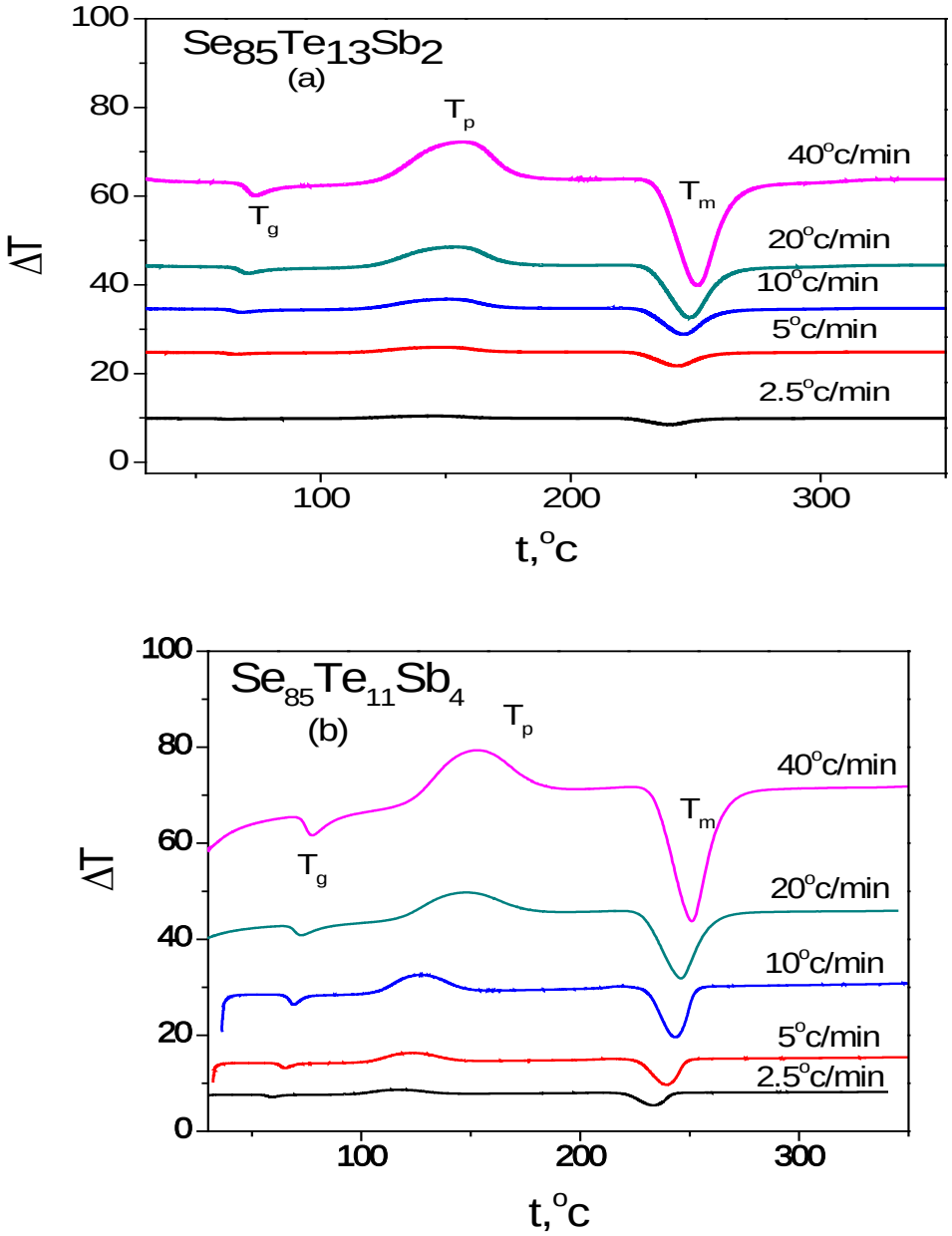

Figs.3(a,b) A typical DSC trace of $Se_{85}Te_{13}Sb_2$ and $Se_{85}Te_{11}Sb_4$ at different heating rates as examples.

Table 2. The values of glass transition temperature (T_g) and the peak crystallization temperature (T_p) at different heating rates for $Se_{85}Te_{15}$, $Se_{85}Te_{13}Sb_2$, $Se_{85}Te_{11}Sb_4$ and $Se_{85}Te_9Sb_6$ glasses.

Heating rate β °C/min	**$Se_{85}Te_{15}$**		**$Se_{85}Te_{13}Sb_2$**		**$Se_{85}Te_{11}Sb_4$**		**$Se_{85}Te_9Sb_6$**	
	T_g, °C	**T_p, °C**	**T_g, °C**	**T_p, °C**	**T_g, °C**	**T_p, °C**	**T_g, °C**	**T_p, °C**
2.5	52.06	107.88	55.4	143	56	145	51.7	156
5	57.26	111.38	59.8	147	61.08	147	54.8	160
10	61.8	116.7	62.9	150	64.6	151	58.1	164
20	64	133.6	64.7	152	66.9	152.88	60.55	165
40	69.3	139.15	69.7	156	71.6	160	63.04	169

The T_g of a multi-component glass is known to be dependent on several independent parameters such as band gap, co-ordination numbers, bond energy, effective molecular weight, the type and fraction of various structural units formed [20-23]. It is interesting to note that T_g varies

with the heating rate β as given in Table 2. It is also clear from Table 2 that T_p increases with increasing heating rate β, so we can say that by increasing the heating rate, the peak crystallization temperature increases due to the reduction in crystal growth. It is also observed that T_p increases with increasing Sb content. On the other hand T_g increases with increasing Sb content up to 4at.wt%%, beyond this at 6 at.wt%% of Sb, T_g decreases. The Sb atom has a larger atomic/ionic radius than Se and Te atoms. Thus, when Sb is added to the Se-Te lattice, the lattice distorts due to the disturbed van der Waal type forces between chains and the rings of the chalcogen atoms [24,25]. The distortion in the lattice gives rise to more three-dimensional disorder in the material .It seems therefore that introduction of Sb in Se-Te system introduces some structural changes. The increase of T_g with initial addition of Sb could be accounted for by cross linking in the chains which increases the chain length thereby enhancing T_g. However, at higher concentration of Sb the structure is broken into a number of chains of smaller lengths due to the larger size of Sb atoms as compared to Se and Te atoms, thus deceasing T_g, which agrees with the conclusions reached by others [2,6,7,23,26].

3.2.1 The activation energy of glass transition E_g

The dependence of T_g on the heating rate β could be discussed using three approaches[7,8].The first approach is the evaluation of activation energy of the glass transition E_g using Kissinger's formula [27, 28]:

$$\ln(\beta / T_g^{\,2}) = -E_g / RT_g + Cons\tan t\,, \qquad (2)$$

Where R is the universal gas constant (R=8.314472 J/K.mole). A plot of $\ln(\beta / T_g^{\,2})$ against $1/T_g$ for the investigated compositions are shown in Fig. (4). The obtained curves are straight lines. The values of the glass transition activation energy (E_g) deduced from the slopes of these lines are listed in Table 3.

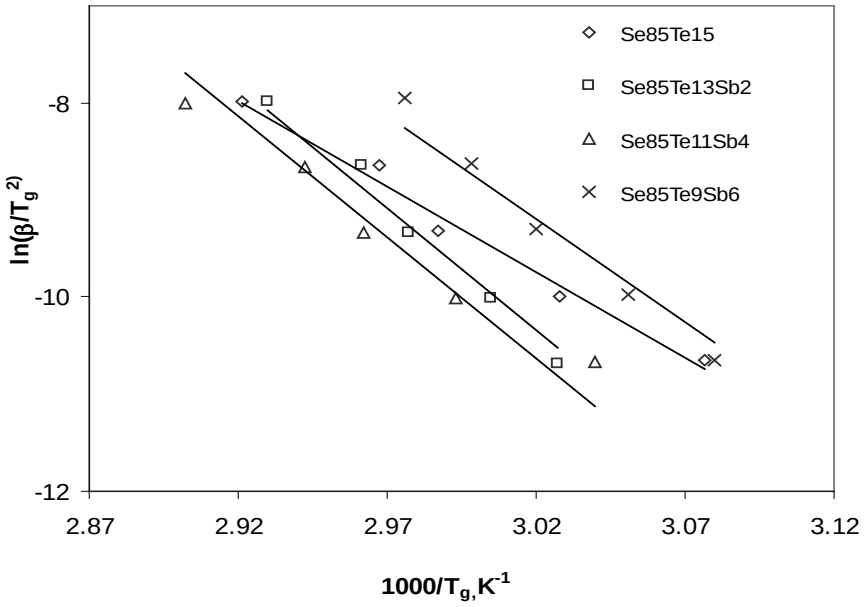

Fig.(4) Variation of $\ln(\beta / T_g^{\,2})$ *against* $1/T_g$ *according to Kissinger formula for* $Se_{85}Te_{15-x}Sb_x$ *(x = 0,2,4&6 at.wt%) glasses.*

Table 3. Values of E_g (k.J.mol^{-1}) for $Se_{85}Te_{15}$, $Se_{85}Te_{13}Sb_2$, $Se_{85}Te_{11}Sb_4$ and $Se_{85}Te_9Sb_6$ according to different methods.

Method	***E_g*, (Kj.mol^{-1})**			
	$Se_{85}Te_{15}$	**$Se_{85}Te_{13}Sb_2$**	**$Se_{85}Te_{11}Sb_4$**	**$Se_{85}Te_9Sb_6$**
Kissinger	147.49	207.26	222.13	176.6
Mahadevan	142.87	204.99	219.84	179.9
Lasocka	*A*=322 *B*=5.28	*A*=323.66 *B*=5.3	*A*=324.74 *B*=5.34	*A*=321.19 *B*=4.10

The second approximation of Mahadevan et .al [29,30] was used, where the variation of $1/T_g^2$ with $ln\beta$ is much slower than that of $1/T_g$ with $ln\beta$; Eq. (2) can be simplified by as follows:

$$\ln(\beta) = -E_g / RT_g + Cons\tan t\,, \tag{3}$$

Fig.(5) shows the plot of $\ln\beta$ against $1/T_g$ for the studied glass compositions. The slope of the resulting straight lines gives (E_g) for the studied samples and listed in Table 3.

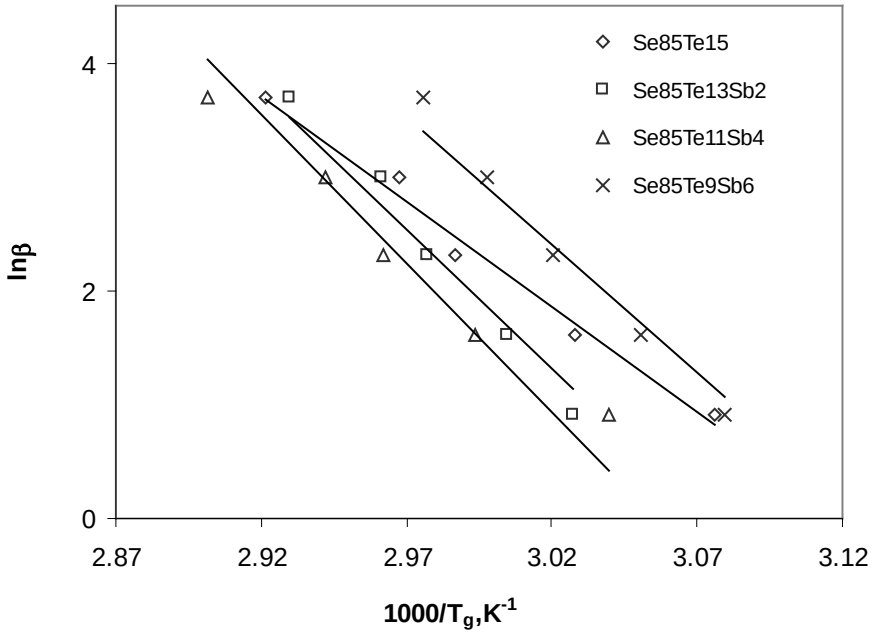

Fig.(5) Variation of $\ln\beta$ against $1/T_g$ according to Mahadevan et al approximation for $Se_{85}Te_{15-x}Sb_x$ (x = 0,2,4&6 at.wt%) glasses.

The third approach is the empirical relation suggested by Lasocka in the form [31,32]:

$$T_g = A + B\ln\beta\,, \tag{4}$$

where *A* and *B* are constants for a given composition. Plots of T_g versus $\ln\beta$ for the investigated glassy compositions are shown in Fig. (6), which confirms the validity of this relation. The obtained values of *A* and *B* are listed in Table 3. It was previously suggested that the value of *B* depends on the glass composition and the quenching rate from the melt, which are the conditions for preparing the compositions under consideration. It is observed from Table 3 that the three methods are in the same order.

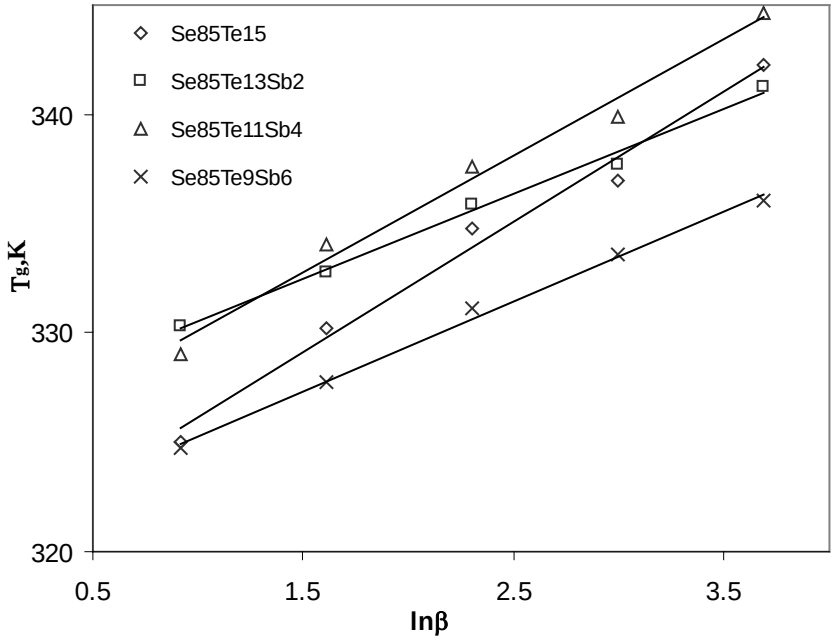

Fig.(6) Plots of T_g *versus* $\ln\beta$ *for* $Se_{85}Te_{15-x}Sb_x$ *(x = 0,2,4&6 at.wt%) glasses.*

It is also clear from this table that E_g increases with increasing Sb content up to 4at.wt% and then decreases as Sb content becomes 6at.wt%. The variation of (E_g) of these glasses can be explained on the basis of structural changes due to the introduction of Sb atoms. It is known that a-Se about 40% of the atoms have a ring structure and 60% of the atoms are bonded as polymeric chains. Tellurium enters as copolymer chains and tends to reduce the number of Se_8 rings [33]. Simultaneously, it increases the number of Se and Te atoms in the chains. The structure of Se-Te system prepared by quenching the melt is regarded as a mixture of Se_8 rings, Se_6Te_2 rings and Se-Te copolymer chains. A strong covalent bond exists between the atoms in the ring whereas in-between chains only Vander Wall's forces are dominant [34-38]. The addition of Sb with small amounts (2-4at.wt%) to Se-Te system leads to its entry into the cross-link chains, and Se-Sb bonds with higher bond energy (214.2kJ/mole) are formed, replacing the Te-Sb bond which has lower bond energy (205.8 kJ/mole) [35] i.e Se_8 ring decreases. As a result the glassy matrix becomes heavily cross-linked and the steric hindrance increases make the structure more rigid [39-42]; it is expected that (E_g) increases with increasing Sb content (2-4%). Further addition of Sb (Sb > 4at.wt%) leads to the formation of Sb-Sb bonds (bond energy176.4 kJ/mole) resulting in decreasing the Se-Sb bond concentration and the concentration of Se_8 rings increases in the glass matrix. The decrease of (E_g) leads to the increasing of the ring concentration, this, in turn, explains the decrease in (E_g) value with the increase of Sb content higher than 4at.wt% [35]. The obtained glasses are stable up to 4at.wt% of Sb content and increasing Sb content leads to the reduction of the system stability.

3.3 .Crystallization

It has been pointed out [43] that in a crystallization process, two types of activation energies have to be considered: activation energy for nucleation E_n and activation energy for growth E_G .The activation energy for the whole crystallization process is called the activation energy of crystallization E_c. Further, it has been shown through various studies [44,45] that the activation energy for growth may be taken equal to the activation energy of whole crystallization E_c .The thermal analysis methods enable the determination of E_c.

The kinetics of phase transformations resulting in a microstructure formation is driven by nucleation and growth steps and in general is well described by Kolmogorov, Johnson, Mehl and

Avrami (KJMA) theory [46,47]. The mixed molecule approach and the empirical theory of glass formation are based on the idea that glass formation is easier when the specific elements mix well and a large number of crystalline stoichiometric compounds are possible between them. This effect reduces the predominance of any one compound therefore, preventing crystallization [48,49]. Nucleation and crystallization rates are sometimes measured directly in the microscope, but differential scanning calorimeter is valuable for the quantitative study of crystallization in different glassy systems.

The activation energies of crystallization E_c for $Se_{85}\ Te_{15-x}\ Sb_x$ glassy system have been estimated using the following methods:

3.3.1Kissinger method: the activation energy for crystallization E_c has been determined for $Se_{85}\ Te_{15-x}\ Sb_x$ (x=0,2,4and 6at.wt%) from the variation of the peak crystallization temperature T_p with the heating rate β using the following equation [50]:

$$\ln(\beta / T_p^{\,2}) = -E_c / RT_p + Cons\tan t\,, \tag{5}$$

where T_p is the peak crystallization temperature

A plot of $\ln(\beta / T_p^{\,2})$ against $1/T_p$ for $Se_{85}Te_{15}$, $Se_{85}Te_{13}\,Sb_2$, $Se_{85}Te_{11}\,Sb_4$ and $Se_{85}Te_9Sb_6$ glasses is shown in Fig. (7). The data were fitted by straight lines. The slope of these straight lines gives the activation energy of crystallization E_c .The estimated values of E_c for all compostions are listed in Table 4 .

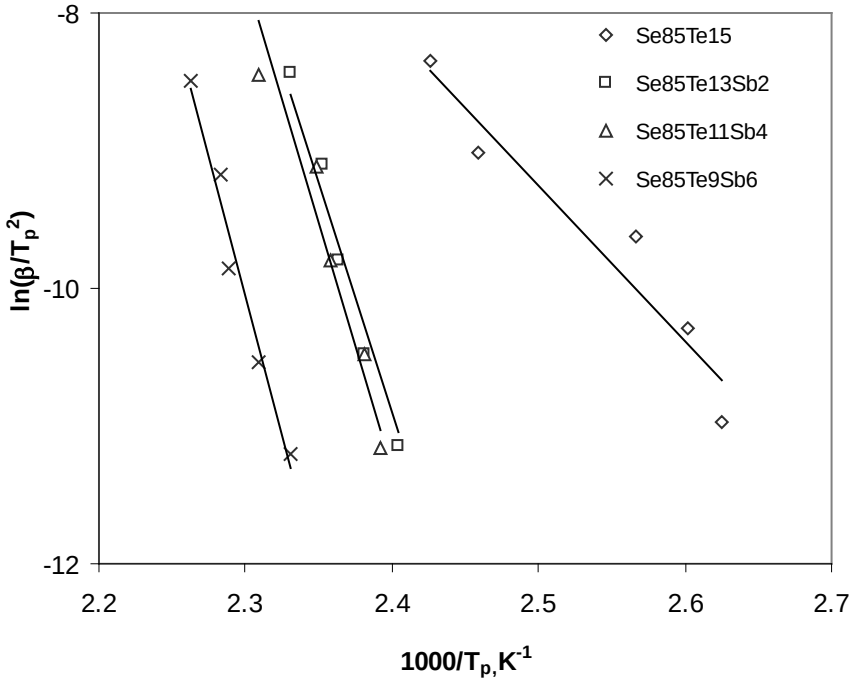

Fig.(7) Plots of $\ln(\beta / T_p^{\,2})$ *against* $1/T_p$ *according to Kissinger formula for* $Se_{85}Te_{15-x}Sb_x$ *(x = 0,2,4&6 at.wt%) glasses.*

Table 4. Values of the crystallization activation energy E_c *for* $Se_{85}Te_{15}$, $Se_{85}Te_{13}\,Sb_2$, $Se_{85}Te_{11}\,Sb_4$ *and* $Se_{85}Te_9Sb_6$ *according to different methods.*

Method	E_c*(k.J .mol^{-1})*			
	$Se_{85}Te_{15}$	$Se_{85}Te_{13}\,Sb_2$	$Sce_{85}Te_{11}\,Sb_4$	$Se_{85}Te_9Sb_6$
Kissinger	93.47	280.17	298.85	335.01
Mahadevan	96.77	276.5	295.15	338.64
Augis and Bennett	100.06	272.83	291.45	339.28

3.3.2.Augis and Bennett method: The crystallization activation energy E_c can also be determined by an approximation method developed by Augis and Bennett, [41,44],which is given as follows:

$$\ln[\beta/(T_p - T_o)] = -E_c / RT_p + \ln k_o \ , \tag{6}$$

Where k_0 is the frequency factor (in S^{-1}) and T_0 is the initial temperature. In the case of $T_p \succ\succ T_o$, the above equation can be approximated as follows [51]:

$$\ln(\beta / T_p \ ) = -E_c / RT_p + Cons\tan t \ , \tag{7}$$

Plots of $\ln(\beta / T_p \ )$ against $1/T_p$ are shown in Fig. (8) for the investigated compositions. From the slope of these lines, the value of the activation energy for crystallization E_c, can be calculated for all compositions which are listed in Table.4.

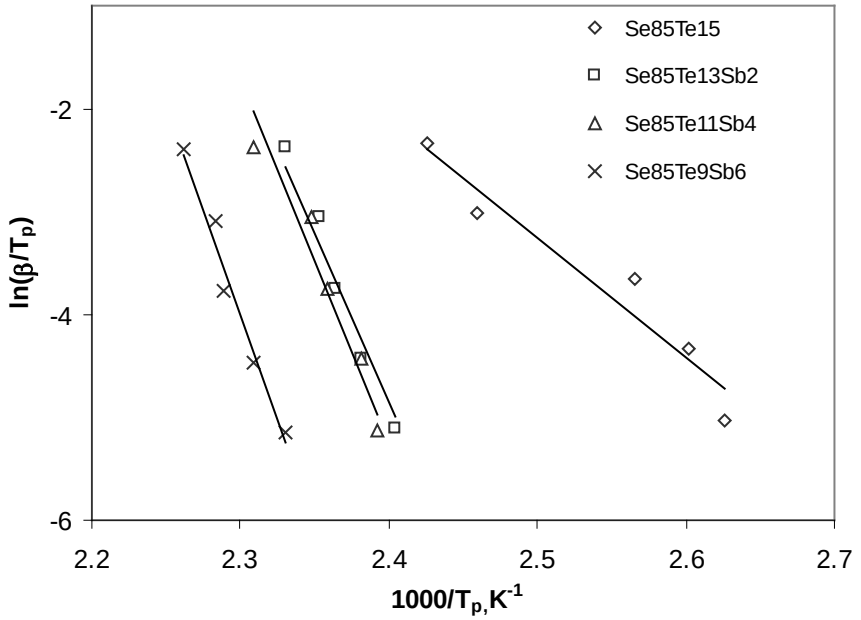

Fig.(8) Plots of $\ln(\beta / T_p)$ *versus* $1/T_p$ *according to Augis and Bennett for for* $Se_{85}Te_{15-x}Sb_x$ *(x = 0,2,4&6 at.wt%) glasses.*

3.3.3The Mahadevan et al method.

The activation energy E_c of crystallization can be determined also by an approximation developed by Mahadevan et al [43,52] according to the following formula:

$$\ln\beta = -E_c / RT_p + Cons\tan t \, , \tag{8}$$

Fig.(9) shows the variation of $\ln\beta$ against $1/T_p$ for the studied compositions. The plot yields straight lines, the slope of which gives the activation energy E_c. The deduced values of E_c for all compositions are listed in Table 4.

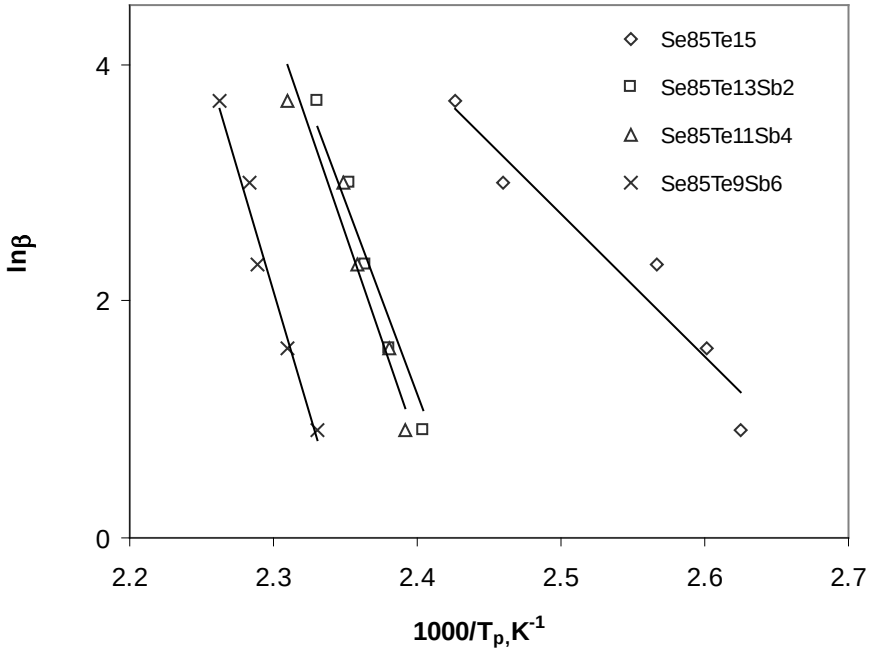

Fig.(9) Plots of $\ln(\beta)$ *versus* $1/T_p$ *according to Mahadevan approximation for* $Se_{85}Te_{15-x}Sb_x$ *(x = 0,2,4&6 at.wt%) glasses.*

It is clear from this table that, the obtained values of E_c, by the three different methods are in agreement with each other for all investigated compositions. It is well known that the activation energy of crystallization is associated with nucleation and growth process that dominates the devitrification of most glassy solids [53-56]. The activation energy of crystallization is an indication of the speed of crystallization rate. It is useful for the characterization of glassy alloys for different applications. It is clear from Table 4 that E_c increases with increasing Sb content in the present system which indicates the speed of crystallization rate, is faster with increasing Sb content [23].

3.3.4.Matusita and Sakka method

Crystallization kinetics has also been studied using a method suggested specially for non-isothermal experiments by Matusita et al.[57,58].In this method the crystallized fraction χ, precipitated in a glass heated at constant rate β, is related to the activation energy for crystallization, E_c through the following expression [59,60]:

$$\ln\{-\ln(1-\chi)\} = -n_c \ln\beta - 1.052 m_c E_c / RT + Cons\tan t, \qquad (9)$$

where m_c and n_c (Avrami index) are integer or half-integer numbers that depend on the growth mechanism and the dimensionality of the crystal. The fraction volume χ crystallized at any temperature T is given as $\chi = A/A_T$, where A_T is the total area of the exotherm between T_i where the crystallization just begins and the temperature T_f where the crystallization is completed and A is the area between T_i and T as shown by the hatched portion in Fig.(2). Here $n_c = m_c+1$ is taken for a quenched glass containing no nuclei and n=m for a preheated glass containing sufficiently large number of nuclei, where m_c is an integer which represents the dimensionality of growth. A plot of $\ln[-\ln(1-\chi)]$ against $1/T_p$ for $Se_{85}Te_{15}$ and $Se_{85}Te_9Sb_6$ as representative examples, measured at different heating rates, give straight lines over most of the temperature range as shown in Figs. 10(a,b).

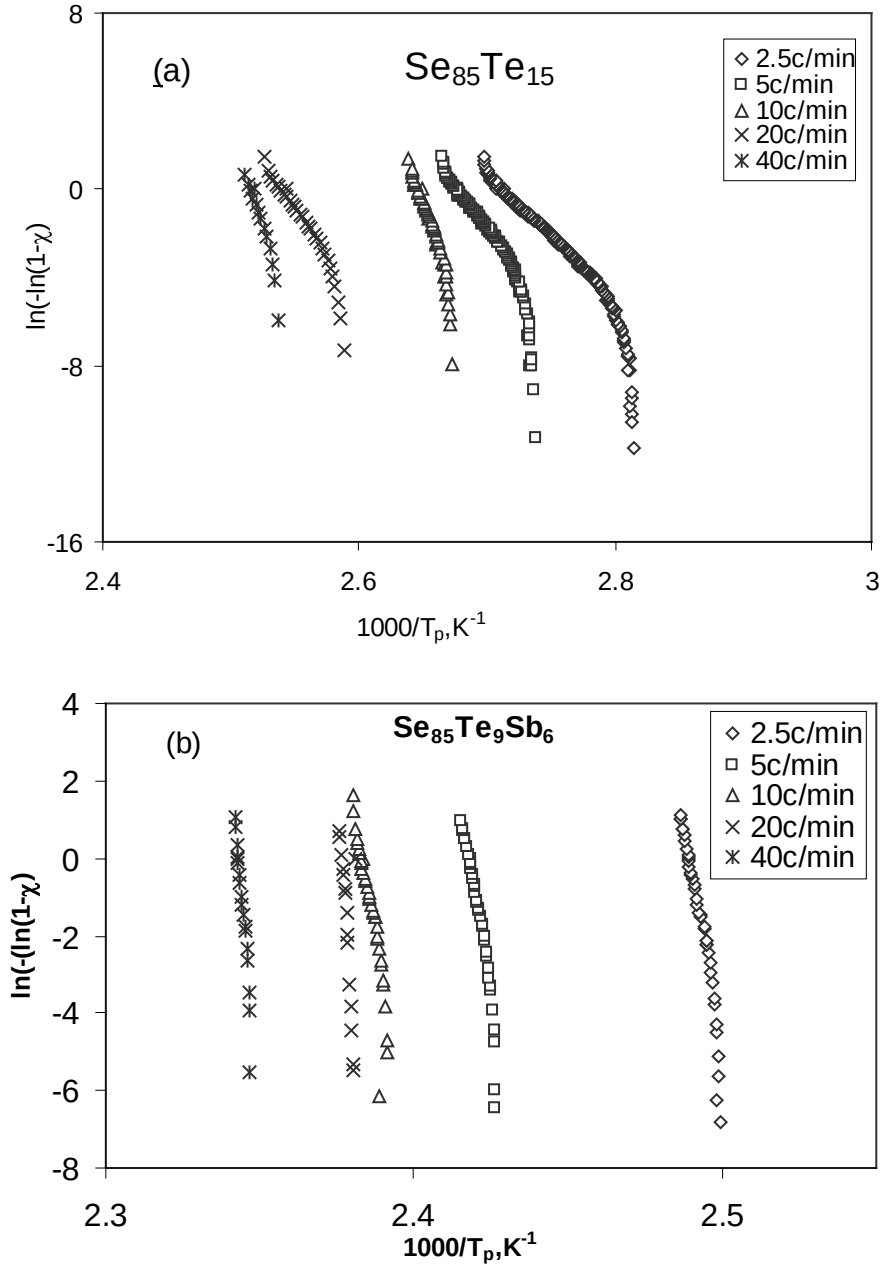

Figs.10(a,b) A plot of $\ln\{-\ln(1-\chi)\}$ *against* $1/T$ *for all the heating rates* β *= 2.5, 5, 10, 20 and 40* $^{O}C/\min$ *for* $Se_{85}Te_{15}$ *and* $Se_{85}Te_9Sb_6$ *glasses.*

It is observed that the plots are linear over a wide temperature range. At higher temperature some deviations from linearity at high temperature or in regions of large crystallized fractions were attributed to the saturation of nucleation sites in the final stages of crystallization [60]. From the slope of each straight line the $(m_c E_c)$ value can be calculated. It seems to be independent on the heating rate, and, therefore, an average value of $(m_c E_c)$ was obtained at the heating rates (β =2.5, 5, 10, 20 and 40 ^{o}C/min). Eq.(9) can be written as :

$$\ln\{-\ln(1-\chi)\} = n\ln\beta + Constant, \qquad (10)$$

Fig.11(a-d) show linear plots of $\ln\{-\ln(1-\chi)\}$ versus $\ln\beta$ at fixed temperature according to Ozwa expression(Eq.(10) [38] for the studied compositions. Using Eq.(10), the values of relations, (Avrami index) n_c, m_c and E_c have been determined and are given in Table 5.

Therefore, the corresponding m_c values are deduced; consequently, the average values of crystallization activation energy E_c were calculated and the above mentioned parameters are listed in Table 5.

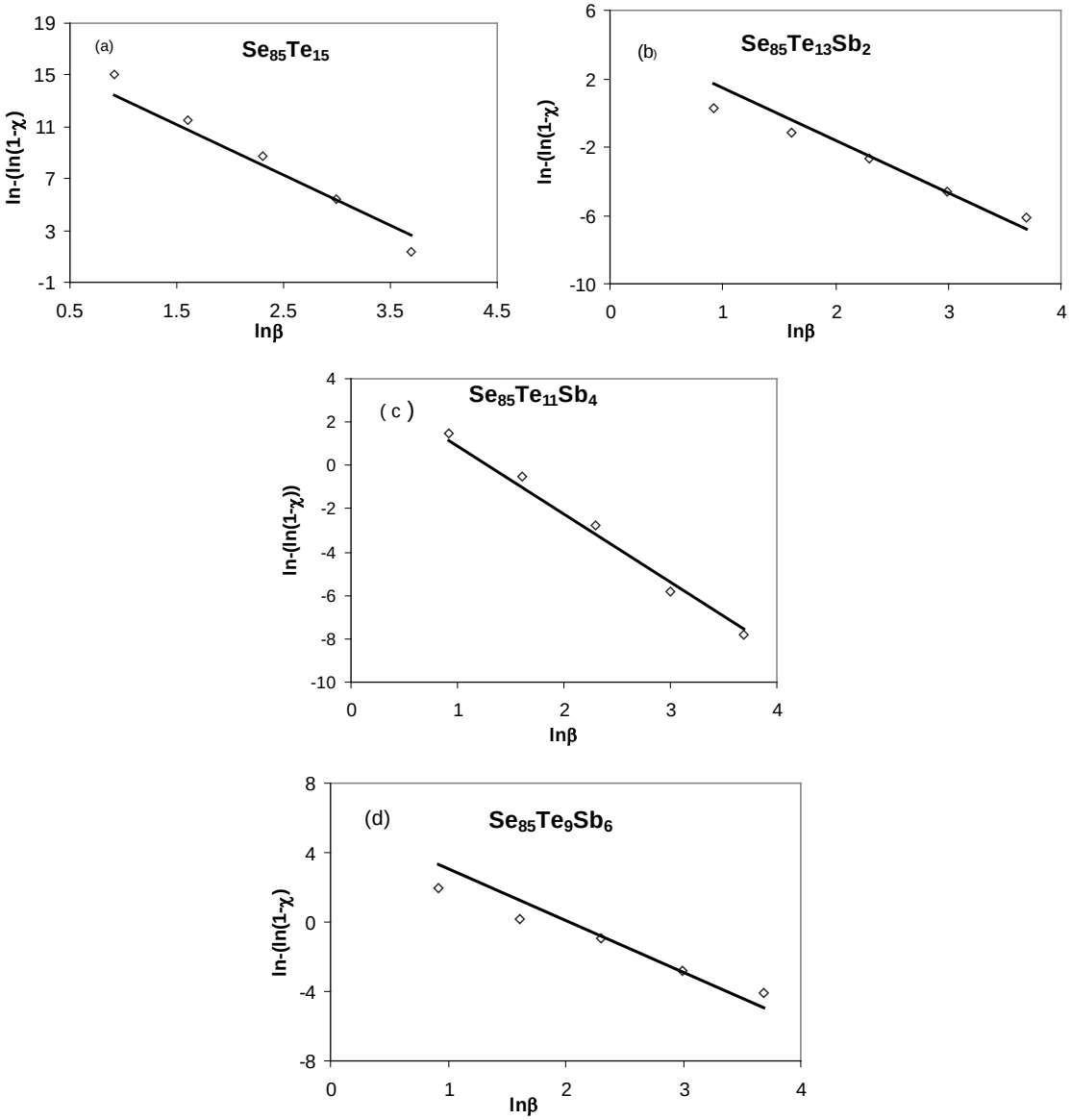

Fig. 11(a-d) Plots of $\ln\{-\ln(1-\chi)\}$ *versus* $\ln\beta$ *according to Avrami for* $Se_{85}Te_{15-x}Sb_x$ *(x = 0,2,4&6 at.wt%) glasses.*

Table 5. Values of E_c (k .J.mol^{-1}), m_c and n_c for $Se_{85}Te_{15}$, $Se_{85}Te_{13}Sb_2$, $Se_{85}Te_{11}Sb_4$ and $Se_{85}Te_9Sb_6$ glasses according to Avrami formula.

Composition	***E_c (k j . mol^{-1})***	***n_c***	***m_c***	***E_c m_c***
$Se_{85}Te_{15}$	206.35	3.01	2.01	621.11
$Se_{85}Te_{13}Sb_2$	252.1	3.060	2.060	519.32
$Se_{85}Te_{11}Sb_4$	298.26	3.080	2.080	620.38
$Se_{85}Te_9Sb_6$	319.02	3.003	2.003	638.99

Since our samples are as quenched, therefore, n_c is considered to equal to m_c+1 and the value of $m_c = n_c$ -1(see Table 5), indicating bulk nucleation with two-dimensional growth in these glasses. [61,62].

4. Conclusions

A systematic investigation of the crystallization kinetics of $Se_{85}Te_{15-x}Sb_x$(x=0,2,4&6at.wt%) chalcogenide glasses has been performed by using non-isothermal DSC measurements. The obtained results suggest that the addition of Sb (2-4 at.wt%) increases the chain length of Se-Te ,resulting in an increase of the glass transition temperature of the alloy, whereas further enrichment in Sb (6at.wt %) leads to a breaking of chains and formation of a larger number of smaller chains with a decrease in the glass transition temperature. It is found also that the peak crystallization temperature increases with increasing Sb content. The observed dependence of heating-rate of the glass transition temperature was discussed in terms of different theoretical models describing glass transition. Difference in values of E_c and E_g using different theoretical models may be attributed to the different approximation used in these models. The results indicate that the crystallization mechanism in Se-Te-Sb glasses occurs in two-dimensional growth according to the obtained values for the Avrami exponent (n_c).

References

[1] Mousa M.A.Imran, Deepika Bhandari, N.S.Saxena, J.Materials Science and Engineering A **292,** 56 (2000).
[2] N. Kushwaha, V.S. Kushwaha, R.K. Shukla, A. Kumar Journal of Non-Crystalline Solids **351**, 3414 (2005).
[3] H. Yinnon, D.R. Uhlmann, J. Non-Cryst. Solids **54**, 253 (1983).
[4] S. Surinach, M.D. Baro, M.T. Clavaguera-Mora, N. Clavaguera, J.Non-Cryst. Solids **58** 209 (1983).
[5] N. Rysava, T. Spasov, L. Tichy, J. Thermal Anal. **32** 1015 (1987).
[6] K.G. Keong,W. Sha, S. Malinov, J. Non-Cryst. Solids **324**, 230 (2003).
[7] C.M. Lee, Y.I. Lin, T.S. Chin, J. Mater. Res. **19**, 2929 (2004).
[8] Y. Zhang, X. Jiang, Y. Guan, A. Zheng, Mater. Lett. **59**, 3626 (2005).
[9] W. Lu, B. Yan,W. Huang, J. Non-Cryst. Solids **351**, 3320 (2005).
[10] J. Holubova, Z. Cernosek, E. Cernoskova, A. Cerna, Mater. Lett. **60**, 2429 (2006).
[11] F. Liu, F. Sommer, C. Bos, E.J. Mittemeijer, Int. Mater. Rev. **52**, 193 (2007).
[12] F. Liu, F. Sommer, E.J. Mittemeijer, J. Mater. Sci. **42**, 573 (2007).
[13] Y.Q. Gao,W.Wang, F.Q. Zheng, X. Liu, J. Non-Cryst. Solids **81**, 135 (1986).
[14] F. Liu, F. Sommer, E.J. Mittemeijer, J. Mater. Sci. **39**, 1621 (2004).
[15] W.W. Wendlandt, Thermal Methods of Analysis, Wiley, New York, 1964.
[16] T. Daniels, Thermal Analysis, Wiley, New York, 1973.
[17] M. Mehdi, G. Brun, J.C. Tedenac, J. Mater. Sci. **30**, 5259 (1995).

[18] M. Kastner, Phys. Rev. Lett. **28**, 355 (1972).
[19] R.M. Mehra, R. Kumar, P.C. Mathur, Thin Solid Films **170**, 15 (1989).
[20] A. Giridhar, S. Mahadevan, J. Non-Cryst. Solids **151**, 245 (1992).
[21] M.K. Rabinal, K.S. Sangunni, E.S.R. Gopal, J. Non-Cryst. Solids **188**, 98 (1995).
[22] S.A. Khan, M. Zulfequar, M. Husain, Solid State Commun. **123**, 463 (2002).
[23] Anis Ahmad, Shamshad A.Khan, A.A.Al-Ghamdi, Faisal A.Al-Agel, Kirti Sinha, M.Zulfequar, M.Husain, J. Alloys and Compounds ,**497** 215 (2010).
[24] A. Von Hippel, J. Chem.Phys **16,** 372 (1948).
[25] K.Vedam,D.L.Miller and R.Roy, J. Appl. Phys **37**, 3432 (1966).
[26]M.F.Kotkata,Sh.A.Mansour,J.Thermal Anal Calorim Doi 10.1007/s10973-010-0963-x(2010).
[27] A.B. Abdel El-Moiz, N. Afify, M. M. Hafiz, Physic B, **182**, 33 (1992).
[28] N. Afify, J. Non-Crst. Solids, **136**, 67 (1991).
[29] S. Mahadevan, A. Giridhar and A. K. Singh, J. Non-Cryst. Solids, **88**, 11 (1986).
[30] A.A. Othman, H.H. Amer, M.A. Osman, A. Dahshan, J. Non-Cryst. Solids, **351**, 130 (2005).
[31] V.S. Shiryaev, J.-L. Adam, X.H. Zhang and M.F. Churbanov, Solid State Sciences, **7**, 209 (2005).
[32] M. Lasocka, Mater. Sci. Engng., **23** 173 (1976).
[33] J. Lucovcy, Mater. Res. Bull. **4** 505 (1996).
[34] P. Predeep, N.S. Saxena, N.B. Maharjan, Phys. Stat. Sol. (a) **189**, 197 (2002).
[35] L.J. Pauling, Nature of the Chemical Bond, Cornell Univ. press, New York, (1960).
[36] M.K. Rabinal, N. Ramesh Rao, K.S. Sangunni, Philos. Mag. **70**, 89 (1994).
[37] P. Pradeep, N.S. Saxena, A. Kumar, J. Phys. Chem. Solids **58,** 385 (1996).
[38] P.K. Dwivedi, Ph.D. thesis, Department of Physics, HBTI, Kanpur, 1996.
[39] A. Giridhar, P.C.L. Narasimham, Sudha Mahadevan, J. Non-Cryst. Solids **43**, 27 (1981).
[40] N.B. Maharjan, D. Bhandari, N.S. Saxena, D.D. Paudyal, M. Hussain, Phys. Stat. Sol. (a) **178**, 663 (2000).
[41] Vibhav K. Saraswat, K.Singh, N.S. Saxena, V. Kishore, T.P. Sharma, P.K. Saraswat, Current applied physics **6**, 14 (2006).
[42]K. Singh, N.S. Saxena, N.B. Maharjan, phys. Stat. Sol. (a) **189**, 197 (2002).
[43] S. Mahadevan, A. Giridhar and A. K. Singh, J. Non-Cryst. Solids, **88**, 11 (1986).
[44] T. Ozawa, Polymer **12**, 150 (1971).
[45] K. Matusita, T. Konatsu, R. Yokota, J. Mater. Sci. **19**, 291 (1984)
[46] A.N Kolmogrov, Isz. Akad. Nauk SSR Ser. Fiz. (1937) 3355.
[47] W.A. Johnson, R. Mehl, Trans. AIME **135**, 416 (1939).
[48] A.R. Hilton, C.R. Jones, M. Brau, Phys. Chem. Glasses **7**, 105 (1966).
[49] S.A. Dembovskii, Izv. Akad. Nauk SSSR. Neorg. Mat. **14**, 803 (1978).
[50] H.E. Kissinger, J. Res. Nat. Bur. Stand. **57**, 331 (1956).
[51] H. Yinnon and D.R. Uhlmann, J. Non-Cryst. Solids, **54**, 253 (1983).
[52] M.A. Abdel-Rahim, A.Y. Abdel-Latif, A. El-Korashy and G.A. Mohamed, J. Mater. Sci. **30**, 5737 (1995).
[53] J. Fusong, X.Yanghu, J.Maguang and G.Fuxi, J. Non-Cryst. Solids, **184**, 51 (1995).
[54] R. Chiba and N. Funakoshi, J.Non-Cryst.Solids, **105**, 105 (1998).
[55] A.K. Petford-Long, R.C. Doole and C.N. Afonso, J. Appl. Phys. **77**, 607 (1995).
[56] L.H. Chou and M.C. Kuo, J. Appl. Phys., **77**, 1964 (1995).
[57] K. Matusita, T. Komatsu, R. Yokota, J. Mater. Sci. **19**, 291 (1984).
[58] R.F. Speyer, S.H. Risbud, Phys. Chem. Glass. **24**, 26 (1983).
[59] M. Avrami, J. Chem. Phys**, 9**, 177 (1941).
[60] N. Afify, J. Non-Cryst. Solids, **142**, 247 (1992).
[61] M.A.Abdel-Rahim, J.Non-Cryst Solids **241** 121 (1998).
[62] A.H. Moharram, A.A. Abu-Sehly, M. Abu El-Oyoun, A.S. Soltan, Physica B **324**, 344 (2002).